Journal of the Ceramic Society of Japan 130 [1] 74-80 2022
DOI http://doi.org/10.2109/jcersj2.21118

JCS-Japan

FULL PAPER

Dependence property of isoelectric points and pH environment on enzyme immobilization on maghemite/hydroxyapatite composite particles

Takeshi YABUTSUKA[1,†], Masaya YAMAMOTO[1] and Shigeomi TAKAI[1]

[1] Department of Fundamental Energy Science, Graduate School of Energy Science, Kyoto University, Yoshida-honmachi, Sakyo-ku, Kyoto 606–8501, Japan

We aimed to establish enzyme immobilization technology using the maghemite/hydroxyapatite (Fe_2O_3/HA) composite particles as enzyme immobilization carriers and to clarify the enzyme adsorption characteristics of the composite particles. Seven kinds of enzymes with various isoelectric points (pI) were immobilized on the Fe_2O_3/HA composite particles in buffered solution adjusted at pH = 7.40 or pH = 10.0, 36.5 °C. Effects of the enzyme pI and the solution pH on the immobilization were investigated. In both of the two kinds of buffered solutions, there was an increase or decrease distribution with a maximum local value for |pH-pI|, which indicated the charge state of the enzymes. The interaction between HA on the composite particles and adsorbed enzymes was expected to be the largest when |pH-pI| = 1–2. It was suggested that α-chymotrypsin, whose adsorbed amount was the most among the seven kinds of the enzymes, in addition, formed a monolayer on the surface of the composite particles in the buffered solution at pH = 7.40, 36.5 °C.

Key-words : Maghemite, Hydroxyapatite, Enzyme immobilization, Isoelectric point, pH environment

[Received July 16, 2021; Accepted September 21, 2021]

1. Introduction

Hydroxyapatite [HA: $Ca_{10}(PO_4)_6(OH)_2$] accounts for ca. 70 % of human biological bones and can exist stably *in vivo* without causing immune reaction due to its affinity, that is, biocompatibility, to the natural bones[1)–4)] and cells.[5),6)] In addition, HA has the property to bond directly with the bone *in vivo*.[7)] For this reason, HA has been applied to artificial bones, artificial tooth roots, and bone replacement agents as a biocompatible material.

Furthermore, HA has the property to adsorb biomolecules such as proteins and enzymes on its crystal surface.[8)] Hydroxyapatite has two crystal planes, *a*-plane and *c*-plane. The *a*-plane is positively charged due to the influence of calcium ions, and the *c*-face is negatively charged due to the influence of phosphate and hydroxyl groups.[9),10)] On the other hand, proteins are positively or negatively charged by charged amino acid residues such as aspartic acid, glutamic acid, lysine, arginine, and histidine. The two crystal planes of the charged hydroxyapatite are thought to adsorb proteins by electrostatically interacting with the charged amino acid residues of proteins.[11)–13)] Using this biomolecular adsorption property, the HA is used as a column packing material for chromatography to separate and purify proteins[8),14),15)] and as a carrier for immobilized enzymes.[12)]

As the temperature and pH of simulated body fluid (SBF)[16),17)] with ion concentrations nearly equal to those of human blood plasma are increased, fine particles of calcium phosphate are precipitate in the solution. Yao et al. found that these particles induced HA formation in SBF in a highly active manner and named them 'apatite nuclei' (ApN).[18)] Various novel bio-functional materials have been developed by forming HA by a biomimetic method combining ApN and SBF. In the previous study, for example, we fabricated HA capsules by attaching ApN to the surface of core materials and immersing them in SBF, in which HA induced by the ApN covered the entire surface of the core materials.[19)]

The Fe_2O_3/HA composite particles, which are HA particles containing maghemite (γ-Fe_2O_3) particles, adsorb enzymes on the surface of the particles by the biomolecule adsorption property of HA and the adsorbed enzymes catalyze chemical reactions. By using γ-Fe_2O_3 particles as the core microparticles and making the HA magnetic, it can be quickly recovered from the solution by magnetic force. By fixing the magnetic apatite capsule with

† Corresponding author: T. Yabutsuka; E-mail: yabutsuka@energy.kyoto-u.ac.jp

‡ Preface for this article: DOI http://doi.org/10.2109/jcersj2.130.P1-1

immobilized enzymes on another material, in addition, further applications such as biosensors and bioreactors can be considered.

In the previous study, we immobilized urease on Fe_2O_3/HA composite particles and fabricated immobilized enzyme capsules for hydrolyzing urea.[20] However, the physical properties and characteristics of the enzyme and the effect of the surrounding environment on the adsorption property of the enzyme have not been clarified. In the previous study, for example, we investigated enzyme immobilization behavior on the Fe_2O_3/HA composite particles and commercially obtained rod-type HA particles in phosphate-buffered saline (PBS).[21] However, it can be predicted that enzyme immobilization behavior should change in different pH environments.

In this study, Fe_2O_3/HA composite particles were fabricated by the biomimetic method using ApN and SBF, and the material properties were evaluated. Then, enzymes were immobilized on the prepared Fe_2O_3/HA composite particles. The enzymes have different properties, such as isoelectric point, and the adsorption properties are expected to be different. In addition, when the pH of the solvent changes, the dissociation state of the carboxy and amino groups of the enzyme also changes. Hence the adsorption properties may also differ depending on the solvent. In this study, therefore, we immobilized seven enzymes with various isoelectric points in PBS at pH 7.40 or carbonate/bicarbonate buffer (CBB) at pH 10.0 and investigated the effects of the isoelectric points of the enzymes and the pH of the solutions on the immobilization.

2. Materials and methods

2.1 Preparation of SBF and ApN

Reagent-grade NaCl, $NaHCO_3$, KCl, $K_2HPO_4{\cdot}3H_2O$, $MgCl_2{\cdot}6H_2O$, $CaCl_2$, and Na_2SO_4 (Fujifilm Wako, Japan) were dissolved in distilled water to the concentrations certified in ISO 23317.[17] Tris-hydroxymethyl-aminomethane (Fujifilm Wako) was added gradually to a final concentration of 50 mM and then adjusted to 36.5 °C, pH = 7.40 with 1 M HCl (Hayashi Pure Chemical, Japan), and the mixture was scale-up to 2 L. Tris-hydroxymethyl-aminomethane was added to 2 L of the prepared SBF again and adjusted to pH = 8.40 at 25.0 °C. Then, ApN were precipitated in the SBF by irradiating with 700 W microwaves for 9 min. Using a nitrocellulose membrane filter (Merck Millipore, USA) with an average pore size of 50 nm, the precipitated ApN were collected by suction filtration. The ApN were washed with 200 mL of distilled water and dried in an incubator at 36.5 °C.

2.2 Fabrication of Fe_2O_3/HA composite particles

To 1 L of distilled water, 30 mg of ApN and 10 mg of γ-Fe_2O_3 particles (Sigma-Aldrich, USA) were added and dispersed by ultrasonication for 10 min. The mixed solution was suction-filtered through a nitrocellulose membrane filter (Merck Millipore, USA) with an average pore size of 0.3 μm, and the γ-Fe_2O_3 particles with attached ApN were collected. The collected γ-Fe_2O_3 particles with attached ApN were added to 1 L of the SBF adjusted at pH = 7.60, 36.5 °C, and dispersed by ultrasonication for 5 min. The mixed solution was placed in a screw vial and shaken by a rotary shaker in an incubator at 36.5 °C for 24 h to produce Fe_2O_3/HA composite particles. The Fe_2O_3/HA composite particles were collected by suction filtration through a nitrocellulose membrane filter with an average pore size of 0.3 μm, washed with distilled water, and dried at 36.5 °C.

2.3 Analyses of Fe_2O_3/HA composite particles

The Fe_2O_3/HA composite particles were evaluated by scanning electron microscopy (SEM: SU6600, Hitachi High-Technologies, Japan), energy dispersive X-ray analyzer (EDX: XFlash® 5010, Bruker, USA), Fourier transfer infrared spectrophotometer (FT-IR; FT-720, HORIBA, Japan) based on the attenuated total reflection method, powder X-ray diffraction (XRD: Ultima IV, Rigaku, Japan) using Cu Kα radiation. In order to measure the molar ratio of calcium to phosphorus (Ca/P) in Fe_2O_3/HA composite particles, the composite particles were dissolved in 1 M nitric acid and subjected to inductively coupled plasma atomic emission spectroscopy (ICP: ICPS-7510, SHIMADZU, Japan).

In order to estimate the collected amount by magnetic force, Fe_2O_3/HA composite particles dispersed in distilled water (2 mg·mL^{-1}) were collected by a neodymium magnet, and the distilled water was removed by decantation. The collected Fe_2O_3/HA composite particles were dried at 36.5 °C and weighed.

2.4 Investigation of immobilization equilibrium time

Fe_2O_3/HA composite particles were added to the prepared PBS to a concentration of 4 mg·mL^{-1} and dispersed by sonication for 5 min. Similarly, the enzyme was dissolved in PBS to 2 mg·mL^{-1} and mixed with the Fe_2O_3/HA composite particles suspension in equal amounts. The mixed solution was stirred at 30.0 °C and 2,000 rpm for 12, 18, and 24 h using a vortex mixer. After stirring, the mixture was centrifuged (2000 rpm, 5 min) and separated into precipitated Fe_2O_3/HA composite particles and supernatant solution. The enzyme concentration in the supernatant was measured by Bradford's method[22] using ultraviolet–visible absorption spectroscopy (U-5100, Hitachi High-Technologies, Japan), and the immobilization efficiency was determined from the following Eq. (1).

$$\text{Immobilization efficiency} = (C_0 - C_1)/C_0 \quad (1)$$

In Eq. (1), C_0 is the initial concentration of the enzyme solution, and C_1 is the concentration of the enzyme remaining in the supernatant.

2.5 Investigation of the effect of pH of the buffer solution

Table 1 shows the list of enzymes used in this study and

their pI. Fe_2O_3/HA composite particles were added to PBS or CBB to a concentration of 4 mg·mL^{-1} and dispersed by sonication for 5 min. Similarly, the enzyme was dissolved in PBS or CBB to 2 mg·mL^{-1} and mixed with the Fe_2O_3/HA composite particles suspension in equal amounts. The mixed solution was stirred at 30.0 °C and 2,000 rpm for 24 h using a vortex mixer. After stirring, centrifugation (2,000 rpm, 5 min) was performed, and the enzyme concentration in the supernatant was measured by the Bradford method to obtain the immobilization efficiency from Eq. (1). The collected Fe_2O_3/HA composite particles were washed with PBS or CBB and dried at 36.5 °C.

2.6 Adsorption isotherm

Fe_2O_3/HA composite particles were added to the prepared PBS to a concentration of 4 mg·mL^{-1} and dispersed by sonication for 5 min. The α-chymotrypsin, which had shown the most immobilization efficiency among the seven enzymes in the test previously described, was dissolved in PBS to become 0.2, 0.4, 0.8, 1.6, 2.0, and 4.0 mg·mL^{-1} and mixed with Fe_2O_3/HA composite particles suspension in equal amounts. The mixed solution was stirred at 30.0 °C and 2,000 rpm for 24 h using a vortex mixer. After stirring, centrifugation (2,000 rpm, 5 min) was performed, and the enzyme concentration in the supernatant was measured by the Bradford method to obtain the immobilization efficiency (I_m) from Eq. (1). The adsorption capacity was determined from Eq. (2).

$$\text{Adsorption capacity } [\text{mg}\cdot\text{g}^{-1}] = C_0 V I_m / m \times 0.01 \quad (2)$$

In Eq. (2), V is the total volume of the mixed solution, and m is the weight of the Fe_2O_3/HA composite particles.

Table 1. Enzymes used in this study

Enzyme	pI	Maker
Pepsin	2.6	Sigma-Aldrich
Invertase	3.8	Sigma-Aldrich
Urease	5.0	Fujifilm Wako
Peroxidase	7.2	Fujifilm Wako
α-Chymotrypsin	8.75	Sigma-Aldrich
Trypsin	10.1	Sigma-Aldrich
Lysozyme	11.0	Fujifilm Wako

3. Results and discussion

Figure 1(a) shows the FT-IR spectra of commercially obtained γ-Fe_2O_3 particles and Fe_2O_3/HA composite particles obtained in this study. In the spectrum of γ-Fe_2O_3 particles, no peaks were observed around 1,000 cm^{-1}. In the spectrum of Fe_2O_3/HA composite particles, new peaks due to P-O stretching vibration were observed around 1,000 cm^{-1} compared to the spectrum of γ-Fe_2O_3 particles. This is a characteristic peak attributed to phosphate groups. Therefore, the Fe_2O_3/HA composite particles were considered to contain phosphate groups indeed, and this was predicted to be derived from HA.

Figure 1(b) shows the powder XRD patterns of commercially obtained γ-Fe_2O_3 particles and Fe_2O_3/HA composite particles obtained in this study. The diffraction pattern of the γ-Fe_2O_3 particles showed several firm peaks attributed to γ-Fe_2O_3. In contrast, the diffraction pattern of the Fe_2O_3/HA composite particles showed new firm peaks, mainly around 26 and 32°, in addition to the peaks of γ-Fe_2O_3. These peaks were attributed to HA and had an overall shape, suggesting that the HA on the obtained Fe_2O_3/HA composite particles had low crystallinity.

Figure 2 shows the SEM image and the EDX spectrum of Fe_2O_3/HA composite particles fabricated in this study. In Fig. 2(a), the needle-like crystals characteristic of HA formed in the SBF formed almost spherical particles. On the other hand, no HA formation was observed by

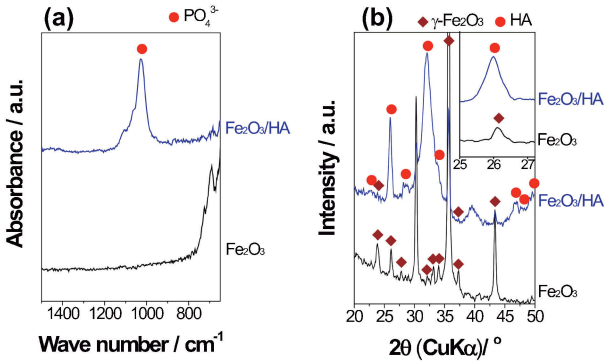

Fig. 1. (a) FT-IR spectra and (b) powder XRD patterns of γ-Fe_2O_3 particles and Fe_2O_3/HA composite particles.

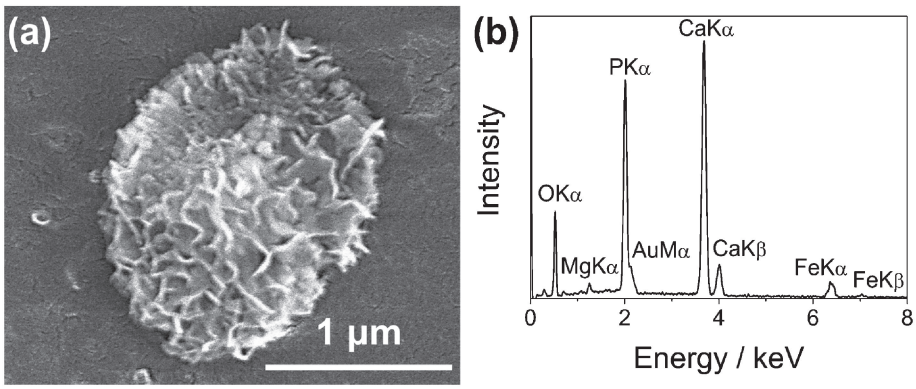

Fig. 2. (a) SEM image and (b) EDX spectrum of Fe_2O_3/HA composite particles.

dispersing only γ-Fe_2O_3 particles in the SBF. Hence, it is considered that HA grew from ApN, which might be agglomerated with γ-Fe_2O_3 particles in the SBF, resulting in spherical particles of 1–2 μm in diameter. In the EDX spectrum of the Fe_2O_3/HA composite particles shown in Fig. 2(b), the iron peak derived from γ-Fe_2O_3 and the calcium and phosphorus peaks derived from HA were observed. The magnesium peak was also detected, suggesting that it is a low-crystalline calcium phosphate with some Ca^{2+} replaced by Mg^{2+}. In the previous study, we fabricated Fe_2O_3/HA composite particles using ApN obtained by raising the pH of SBF to 8.60, 25.0 °C without raising the temperature.[20] In this study, we fabricated them using ApN by raising the pH of SBF to 8.40 and subsequently raising the temperature by microwave. However, the material morphology of the Fe_2O_3/HA composite particles was not so changed only by changing the ApN preparation condition in this experimental system. Hence, it is considered that the HA formation ability of both the ApN was not so different.

The average Ca/P molar ratio of the Fe_2O_3/HA composite particles was calculated at 1.46. It was reported that the Ca/P molar ratio of calcium-deficient apatite is ca. 1.5,[23),24)] and the Fe_2O_3/HA composite particles prepared in this study showed an almost similar level. Therefore, the HA in the Fe_2O_3/HA composite particles is considered to be low-crystalline calcium-deficient HA.

The collection ratio of Fe_2O_3/HA composite particles by neodymium magnet was measured, and 90.0 ± 4.7 % of Fe_2O_3/HA composite particles could be collected. Therefore, it was shown that the Fe_2O_3/HA composite particles could be collected by magnetic force without being shielded by the HA covered on the surface of the composite particles. This result suggested that the Fe_2O_3/HA composite particles can be available for enzyme immobilization carriers by adsorption of enzymes on HA and collection of the enzyme-adsorbed particles in magnetic fields by the magnetism of γ-Fe_2O_3.

Figure 3 shows the time characteristics of the immobilization efficiency of various enzymes with different pI in PBS. The immobilization efficiency of all kinds of enzymes increased after 12 h, and the immobilization reached equilibrium within 24 h in the experimental system in this study. After equilibrium, α-chymotrypsin showed the most immobilization amount among the seven kinds of enzymes. In contrast, pepsin, peroxidase, and lysozyme showed less than 20 % of immobilization efficiency. This result shows that immobilization efficiency was vastly different depending on the kinds of enzymes. In the previous study, we investigated urease immobilization on Fe_2O_3/HA composite particles by investigating the amount of nickel, which exists an active center of urease, using inductively coupled plasma atomic emission spectroscopy.[20] This study showed a similar level of urease immobilization.

Figure 4(a) shows the immobilization efficiency of the enzyme on Fe_2O_3/HA composite particles in PBS. The abscissa is the pI of the enzyme. When the pI was lower than 6, the immobilization efficiency increased as the pI increased. When the pI was higher than 8, in contrast, the immobilization efficiency decreased as the pI increased. When the pI was ca. 7, which was almost the same value as the initial solution pH, the immobilization efficiency was considerably low. In other words, immobilization efficiency was not linearly changed depending on the increase of the pI. This phenomenon was contrary to our initial expectations.

Figure 4(b) shows the immobilization efficiency of the enzymes immobilized on Fe_2O_3/HA composite particles in CBB. The abscissa is the pI of the enzyme similar to Fig. 4(a). By changing the pH of the solution from 7.40 to 10.0, it can be seen that the immobilization efficiency of each enzyme was respectively changed. Even in CBB, however, the immobilization efficiency did not change linearly depending on the enzyme pI, similar to the case of PBS. When the pI was lower than 9, the immobilization efficiency increased as the pI increased. When the pI was ca. 10, which was almost the same value as the initial solution pH, the immobilization efficiency became considerably low. When the pI was higher than 11, the immobilization efficiency increased in comparison with pI $\sim$ 10. For both in the case of PBS and CBB, it can be seen that immobilization efficiency increased as pI was close to solutions pH. When the pI was too close to the initial pH, however, the immobilization efficiency became considerably low in the case of both PBS and CBB. In order to clarify the correlation of the pI and the immobilization efficiency more clearly, we introduced another estimative index.

Tables 2 and **3** show the results of the pH measurement of the enzyme solution. Because the enzyme is a high-molecular compound consisting of amino acids, it has many dissociating groups and polar groups, and its charge state differs depending on the pH. In an enzyme solution at pH = pI, the sum of the positive and negative charges of the enzyme is zero, and the solution is electrically neutral. The closer the value of |pH-pI| is to zero, the closer the pH of the solution is to the pI, and the more electrically neutral the enzyme is. Conversely, the larger the value of |pH-pI|, the more strongly the enzyme is charged.

Figure 5(a) shows the immobilization efficiency of enzymes immobilized on Fe_2O_3/HA composite particles in PBS, where the abscissa is |pH-pI|. The immobilization efficiency did not linearly increase or decrease with the increase of |pH-pI|. The immobilization efficiency was small when |pH-pI| was close to 0, reached a maximum when |pH-pI| = 1.74, and then decreased as |pH-pI| increased from |pH-pI| = 1.74 to a higher value. These results suggest that the immobilization of enzymes on Fe_2O_3/HA composite particles was not only dominated by the interaction of the electric double layer but also occurred due to various factors such as van der Waals forces and local ionic interactions. In other words, it is considered that the effect of the electric double layer of the carrier particles was only a partial factor governing the enzyme adsorption. In the previous study, in addition, we have clarified that similar phenomena, that is, the above relationship between

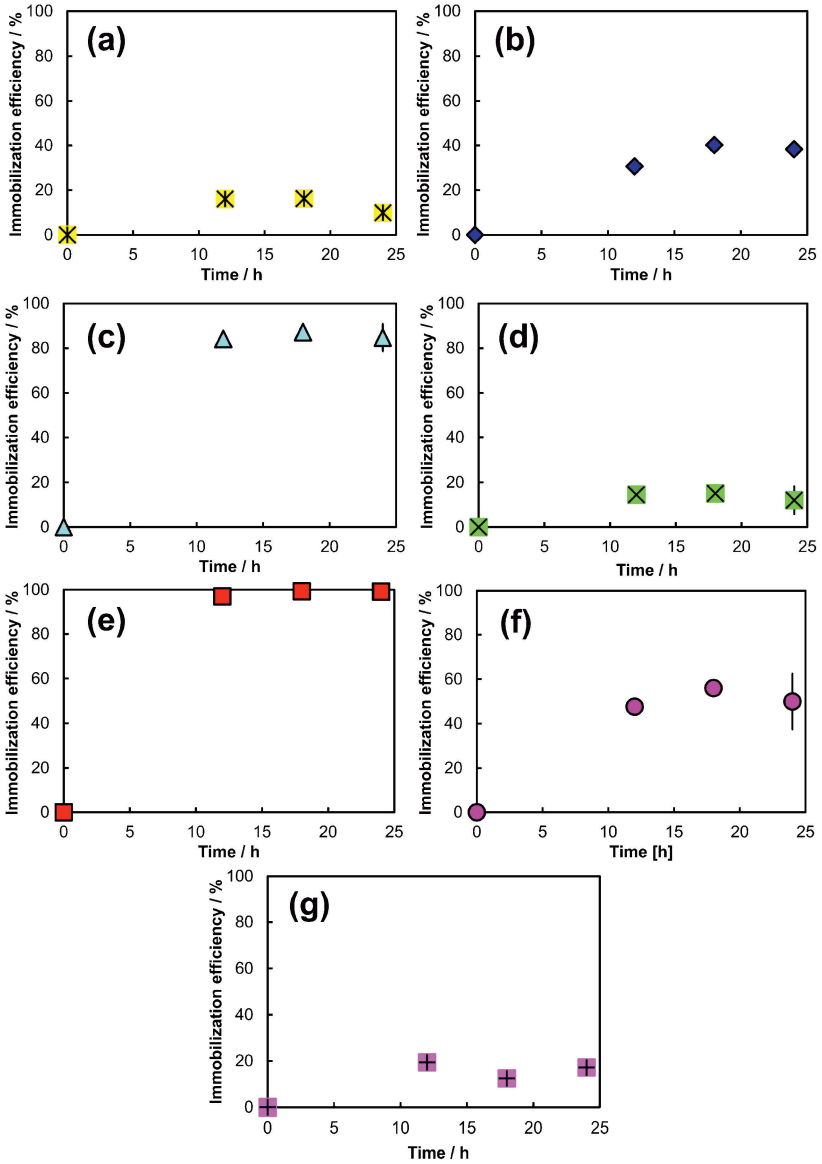

Fig. 3. Immobilization efficiencies of (a) pepsin, (b) invertase, (c) urease, (d) peroxidase, (e) α-chymotrypsin, (f) trypsin and (g) lysozyme on Fe_2O_3/HA composite particles in PBS.

the immobilized amount and |pH-pI|, were also shown on the commercially obtained rod-type HA particles.[21] Hence, it is considered that such a tendency of enzyme immobilization from the viewpoint of isoelectric points was tightly related to the interactions between the HA surface and enzymes.

Figure 5(b) shows the immobilization efficiency of enzymes immobilized on Fe_2O_3/HA composite particles in CBB. The abscissa is set as |pH-pI| similar to the case of PBS. When the abscissa was set as |pH-pI|, the same tendency as in the case of PBS was observed: α-chymotrypsin (|pH-pI| = 1.74 in PBS) was immobilized the most in PBS, and α-chymotrypsin (|pH-pI| = 1.27 in CBB) was immobilized the most in CBB, too, suggesting that |pH-pI| = 1–2 was maximum local value for the enzyme immobilization efficiency. In other words, the interaction between Fe_2O_3/HA composite particles and enzymes is considered to be the largest when |pH-pI| = 1–2. In contrast, it is considered that the interaction was considerably low when pH∼pI. Hence, the enzymes with low immobilization efficiency in this experimental system might show high ones by using solvents that make |pH-pI| = 1–2.

Figure 6(a) shows the adsorption isotherm of α-chymotrypsin, which showed the most immobilization efficiency among the seven kinds of enzymes on Fe_2O_3/HA composite particles in PBS. The adsorption capacity (q_e) increased with increasing equilibrium concentration (C_e) and gradually reached saturation. Such types of adsorption isotherm are so-called the Langmuir type, and it is assumed that monolayer adsorption occurred. Based on Langmuir's equation, the ordinate in Fig. 6(a) was converted from q_e to C_e/q_e, and we re-plotted it in Fig. 6(b). Because the R^2 value of the approximate line was close to

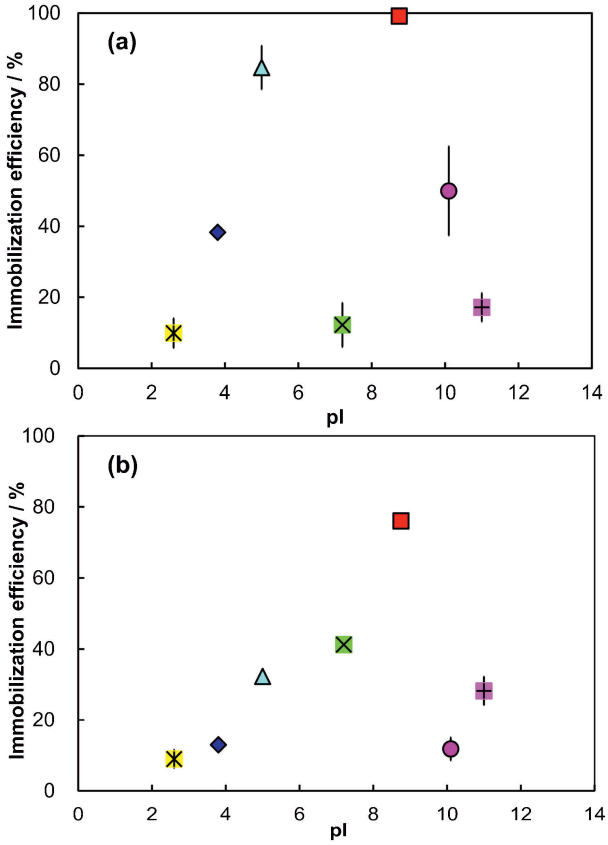

Fig. 4. Dependence property between immobilization efficiency on Fe_2O_3/HA composite particles and pI of enzymes used in this study in (a) PBS and (b) CBB. Each symbol shows the kinds of enzymes and is corresponded to that in Fig. 3.

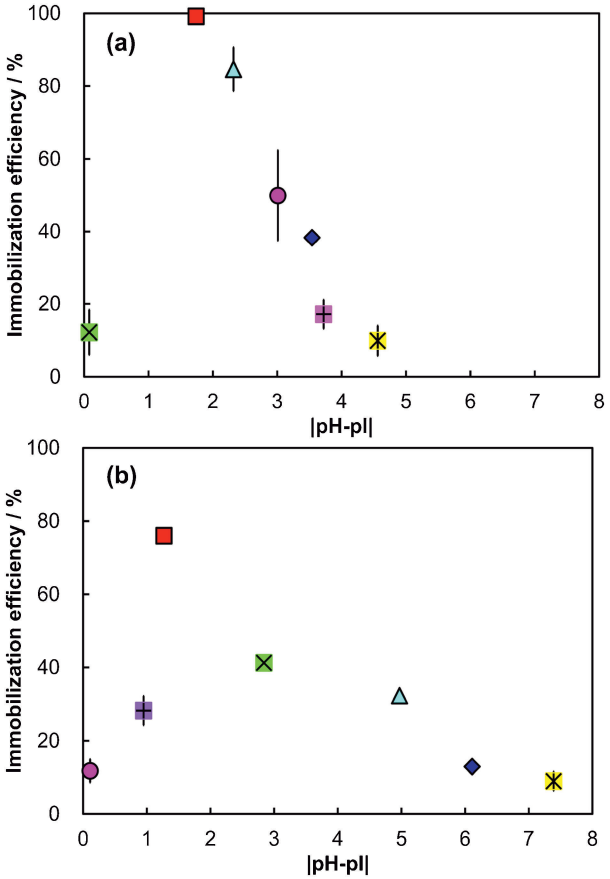

Fig. 5. Dependence property between immobilization efficiency and |pH-pI| of enzymes used in this study in (a) PBS and (b) CBB. Each symbol shows the kinds of enzymes and is corresponded to that in Fig. 3.

Table 2. pH and |pH-pI| in enzyme dispersed PBS

Enzyme	pH	|pH-pI|
Pepsin	7.16	4.56
Invertase	7.34	3.54
Urease	7.32	2.32
Peroxidase	7.28	0.08
α-Chymotrypsin	7.01	1.74
Trypsin	7.09	3.01
Lysozyme	7.28	3.72

Table 3. pH and |pH-pI| in enzyme dispersed CBB

Enzyme	pH	|pH-pI|
Pepsin	9.99	7.39
Invertase	9.91	6.11
Urease	9.97	4.97
Peroxidase	10.04	2.84
α-Chymotrypsin	10.02	1.27
Trypsin	9.99	0.11
Lysozyme	10.05	0.95

1, it is speculated that α-chymotrypsin formed a monolayer on the surface of the Fe_2O_3/HA composite particles.

We acknowledge the several limitations in this report. First, we used only two kinds of buffered solutions at pH 7.40 or pH 10.0 in this study. In order to clarify the correlation of the immobilization efficiency, pH and pI more deeply, immobilization tests using buffers at various pH should be carried out. In addition, the relationship between immobilization efficiency and activity of enzymes with various isoelectric points has not been investigated in this study. The previous study examined the urease activity immobilized on the Fe_2O_3/HA composite particles.[20] Although the decomposition speed of urea was slower than the not-immobilized urease, it was clarified that the immobilized urease decomposed urea almost entirely in the aqueous solution.[20] However, the activity of the immobilized other enzymes, such as basic protein, has not been investigated yet. The relationship between enzyme activity after the immobilization and their isoelectric points is an essential factor for utilization for enzyme immobilization technology. These points will be clarified in a future study.

4. Conclusion

We fabricated the Fe_2O_3/HA composite particles with magnetism. The immobilization efficiency of the enzyme on the Fe_2O_3/HA composite particles did not show a strong correlation with the isoelectric point. The immobilization efficiency did not increase or decrease linearly with the increase of |pH-pI| but reached a maximum at α-chymotrypsin and then decreased with the increase of

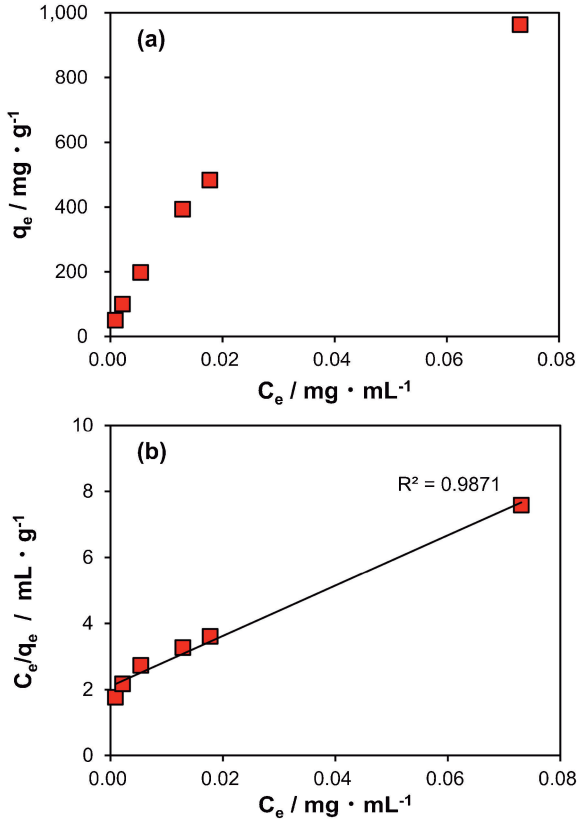

Fig. 6. (a) Adsorption isotherm and (b) Langmuir's plots of α-chymotrypsin on Fe_2O_3/HA composite particles in PBS.

|pH-pI|. This suggested that the immobilization of the enzyme on HA was not dominated by the interaction of the electric double layer but was caused by various factors such as van der Waals forces and local ionic interactions. The immobilization efficiency of α-chymotrypsin was the highest for both solvents at pH = 7.40 and pH = 10.0, 36.5 °C, where |pH-pI| = 1–2. This suggested that the interaction between the HA and the enzyme is the largest when |pH-pI| = 1–2. The prepared Fe_2O_3/HA composite particles showed the possibility of immobilizing various kinds of enzymes with high efficiency by using solvents that make |pH-pI| = 1–2. Alpha-chymotrypsin, which showed the most immobilization efficiency, was suggested to form a monolayer on the Fe_2O_3/HA composite particles in PBS. This study is expected to be helpful for contributing to the development of novel enzyme immobilization carriers with both enzyme affinity and collection advantage by magnetism.

Acknowledgments This work was partly supported by Kansai Research Foundation for Technology Promotion, Japan.

References

1) M. J. Jarcho, J. L. Kay, R. H. Gumaer and H. P. Drobeck, *J. Bioeng.*, 1, 79–92 (1977).
2) R. Z. LeGeros and J. P. LeGeros, in "An Introduction to Bioceramics", Ed. by L. L. Hench, Imperial College Press, London (2013) pp. 229–277.
3) R. Z. LeGeros and J. P. LeGeros, in "Bioceramics and Their Clinical Applications", Ed. by T. Kokubo, Woodhead Publishing, Cambridge (2008) pp. 367–394.
4) H. Oonishi, H. Oonishi, Jr. and S. C. Kim, in "Bioceramics and Their Clinical Applications", Ed. by T. Kokubo, Woodhead Publishing, Cambridge (2008) pp. 606–687.
5) D. D. Deligianni, N. D. Katsala, P. G. Koutsoukos and Y. F. Missirlis, *Biomaterials*, 22, 87–96 (2001).
6) S. C. Rizzi, D. J. Heath, A. G. A. Coombes, N. Bock, M. Textor and S. Downes, *J. Biomed. Mater. Res.*, 55, 475–486 (2001).
7) M. Jarcho, *Clin. Orthop. Relat. R.*, 157, 259–278 (1981).
8) A. Tiselius, S. Hjerten and O. Levin, *Arch. Biochem. Biophys.*, 65, 132–155 (1956).
9) T. Kawasaki, S. Takahashi and K. Ikeda, *Eur. J. Biochem.*, 152, 361–371 (1985).
10) T. Kawasaki, K. Ikeda, S. Takahashi and Y. Kuboki, *Eur. J. Biochem.*, 155, 249–257 (1986).
11) E. Mavropoulos, A. M. Costa, L. T. Costa, C. A. Achete, A. Mello, J. M. Granjeiro and A. M. Rossi, *Colloid Surface B*, 83, 1–9 (2011).
12) Y. Ma, J. Zhanga, S. Guo, J. Shi, W. Du, Z. Wang, L. Ye and W. Gu, *Mat. Sci. Eng. C-Mater.*, 68, 551–556 (2016).
13) A. Oyane, T. Ootsuka, K. Hayama, Y. Sogo and A. Ito, *Acta Biomater.*, 7, 2969–2976 (2011).
14) J. A. S. Bett, L. G. Christner and W. K. Hall, *J. Am. Chem. Soc.*, 89, 5535–5541 (1967).
15) H. Hirano, T. Nishimura and T. Iwamura, *Anal. Biochem.*, 150, 228–234 (1985).
16) T. Kokubo and H. Takadama, *Biomaterials*, 27, 2907–2915 (2006).
17) ISO 23317, Implants for surgery — In vitro evaluation for apatite-forming ability of implant materials (2014).
18) T. Yao, M. Hibino, S. Yamaguchi and H. Okada, U.S. Patent, 8178066 (2012), Japanese Patent, 5261712 (2013).
19) T. Yabutsuka, *Bull. Ceram. Soc. Jpn.*, 53, 819–822 (2018).
20) T. Yabutsuka, S. Kumazawa and S. Takai, *J. Ceram. Soc. Jpn.*, 128, 883–889 (2020).
21) M. Yamamoto, T. Yabutsuka, S. Takai and T. Yao, *T. MRS Jap.*, 43, 153–156 (2018).
22) M. Bradford, *Anal. Biochem.*, 72, 248–254 (1976).
23) R. M. Wilson, J. C. Elliott, S. E. P. Dowker and L. M. Rodriguez-Lorenzo, *Biomaterials*, 26, 1317–1327 (2005).
24) N. Ohtsu, S. Hiromoto, M. Yamane, K. Satoh and M. Tomozawa, *Surf. Coat. Tech.*, 218, 114–118 (2013).